Can. J. Remote Sensing, Vol. 32, No. 6, pp. 367–379, 2006

Interpretation of landscape structure gradients based on satellite image classification of land cover

Julia Linke and Steven E. Franklin

Abstract. Landscape metrics used to quantify landscape structure and pattern over time and space are increasingly required in wildlife habitat analysis and other applications in environmental management, planning, and research. In such analyses, the spatial attributes of either individual land cover classes or the entire landscape mosaic consisting of multiple land cover classes can be described by computing the respective class- and landscape-level landscape metrics. Recent studies have suggested that a parsimonious suite of independent landscape metrics, or *landscape structure gradients*, may be useful descriptors of spatial variation over various natural landscapes and that some of these parsimonious gradients may be fundamental to most landscape configurations as guided by the universality of the gradients (percentage of landscape or land cover classes a structure gradient occurs in), consistency (the correlation of principal component loadings of like-structure gradients across different land cover classes), and strength (average variance explained by the structure gradient across land cover classes). Landscape structure gradients can be extracted using separate principal components analyses of a list of class- and landscape-level landscape metrics obtained from land cover maps derived from geographic information system (GIS) databases or remote sensing image classifications. In this study, we examined the landscape structure gradients in the Foothills Model Forest, which is located in the Canadian Rocky Mountains Yellowhead Ecosystem, Alberta, Canada, and interpreted differences in quantified gradients of landscape structure using satellite image classification products before and after they were generalized into "polygon-like" maps by smoothing. We used 195 square (5.4 km × 5.4 km) sub-landscapes to ensure an adequate sample size for statistical testing. The class-level analysis resulted in the identification of five consistent structure gradients universally present across the eight land cover classes together explaining the majority of all class-level variation (on average about 53% for all land cover classes). The landscape-level analysis identified that a parsimonious suite of eight fundamental landscape-level structure gradients explained approximately 85% of the variance.

Résumé. Les métriques du paysage utilisées pour la quantification de la structure et des patrons du paysage dans le temps et l'espace sont de plus en plus nécessaires pour l'analyse des habitats fauniques et les autres applications en gestion, planification et recherche environnementales. Dans de telles analyses, les attributs spatiaux soit des classes individuelles de couvert soit de la mosaïque complète du paysage comprenant plusieurs classes de couvert peuvent être décrits en compilant les métriques du paysage à la fois au plan des classes et du paysage même. Des études récentes ont indiqué qu'une série simple de métriques indépendantes du paysage, ou gradients de structure du paysage, peut constituer un ensemble de descripteurs utiles de la variation spatiale à travers divers paysages naturels et que certains de ces gradients simples peuvent être fondamentaux par rapport à la plupart des configurations du paysage tel que guidé par l'universalité (pourcentage de classes de paysage ou de couvert où un gradient de structure se manifeste), la cohérence (la corrélation des poids des composantes principales des gradients de type structure à travers différentes classes du couvert) et la puissance (variance moyenne expliquée par le gradient de structure à travers les classes du couvert) des gradients. Les gradients de structure du paysage peuvent être extraits à l'aide d'analyses en composantes principales séparées à partir d'une liste de métriques du paysage au niveau des classes et du paysage obtenues à partir des cartes du couvert dérivées des bases de données SIG ou des classifications d'images de télédétection. Dans cette étude, nous avons examiné les gradients de structure du paysage dans la Forêt modèle de Foothills, située dans l'écosystème Yellowhead des Rocheuses canadiennes, en Alberta, au Canada, et interprété les différences dans les gradients quantifiés de structure du paysage à l'aide des produits de classification d'images satellitaires avant et après que ceux-ci furent généralisés sous forme de cartes de type polygone par lissage. Nous avons utilisé 195 sous-paysages de forme carrée d'une dimension de 5,4 km pour assurer une taille d'échantillon adéquate pour les tests statistiques. L'analyse au niveau de la classe a mené à l'identification de cinq gradients de structure cohérents présents de façon universelle à travers les huit classes du couvert expliquant ensemble la majorité de la variation de toutes les classes (en moyenne 53 % de toutes les classes du couvert). L'analyse réalisée au niveau du paysage a permis d'identifier qu'une série simple de huit gradients de structure du paysage de base expliquait environ 85 % de la variance.
[Traduit par la Rédaction]

Received 20 April 2005. Accepted 24 November 2006.

J. Linke.[1] Department of Geography, University of Calgary, Calgary, AB T2N 1N4, Canada.

S.E. Franklin. Department of Geography, University of Saskatchewan, Saskatoon, SK S7N 4P3, Canada.

[1]Corresponding author (e-mail: jlinke@ucalgary.ca).

Introduction

The relationships between spatial patterns of land cover quantified by landscape metrics and wildlife habitat have emerged in recent years as an important application of remote sensing and geographic information system (GIS) data (Wiens, 1989; Levin, 1992; Diaz, 1996; Davidson, 1998). Specific landscape metrics, such as mean patch size and edge density, have been related to habitat use and habitat selection for several wildlife species (Stuart-Smith et al., 1997; Chapin et al., 1998; Knutson et al., 1999; Potvin et al., 2001; Linke et al., 2005). In such analyses, the spatial composition and configuration can be described either for individual land cover classes by computing class-level landscape metrics (e.g., mean patch size equal to 40 ha for forest patches and 15 ha for clearcut patches) or for the entire landscape mosaic consisting of multiple land cover classes by computing landscape-level landscape metrics (e.g., mean patch size of entire landscape equal to 25 ha) (McGarigal et al., 2002). These studies and others have suggested that landscape metrics are ecologically important quantitative tools but have also identified a number of problems in their derivation and use. For example, it is not at all clear, despite numerous individual studies, what the impact of specific map input characteristics might have on a landscape metric analysis. Three of the most pressing problems when selecting a landscape metric approach can be summarized as follows: (*i*) appropriate spatial data, with emphasis on appropriate grain, extent, and classification scheme, must be developed from which the large number of landscape metrics can be extracted (McGarigal and Marks, 1995; Frohn, 1998; Franklin et al., 2000; McGarigal et al., 2002); (*ii*) attempts to compare landscape metrics of the same place from different map inputs and times may be constrained by differences in map resolution and accuracy (Franklin et al., 2002); and (*iii*) it has been widely acknowledged that many landscape metrics may be redundant (Riitters et al., 1995).

To address these issues and others, the identification of a parsimonious suite of landscape metrics that describe major independent gradients of landscape structure and that are consistent across various natural landscapes could be suggested. It is thought that the landscape structure may be characterized by a few groups of metrics or *landscape structure gradients* (McGarigal and McComb, 1995; Riitters et al., 1995; S. Cushman, K. McGarigal, and M.C. Neel, personal communication, 2002). These gradients measure the major independent dimensions of landscape structure and may provide a standardized reference for quantitative comparison among different landscapes even in cases when different geospatial technologies are used (e.g., where individual metrics may vary greatly depending on the type of mapping involved in the comparison). Landscape structure gradients may be relatively insensitive to such variation and could in this way facilitate comparisons across landscapes. For example, a preliminary parsimony analysis was undertaken on 54 landscape-level metrics and 49 class-level metrics ("Pland" was not counted here since it only served statistical purposes during principal component analysis) in three separate regions of North America (western Massachusetts, southwestern Colorado, and central Idaho) by the Massachusetts Landscape Ecology Program (MLEP; available from http://www.umass.edu/landeco/). Based on polygon-based, GIS land cover maps, S. Cushman, K. McGarigal, and M.C. Neel (personal communication, 2002) have suggested that as few as seven class-level and eight fundamental landscape-level structure gradients could be derived, which are universal, consistent, and strong descriptors of the spatial attributes of the various landscape patterns across the different regions. These fundamental, common landscape structure gradients may be present with other strong and consistent but idiosyncratic structure gradients unique to the specific land cover classes or regions (McGarigal, 2003) that constitutes an important recognition in the metric selection process if the total spatial variability is to be described.

In this study, we identified independent class- and landscape-level structure gradients in the Foothills Model Forest study area, located in the Alberta Rocky Mountains. The application of landscape metrics is of interest in this area because of the possible use in understanding and monitoring grizzly bear population and ecosystem health (Stenhouse and Munro, 2000). Our goal was to test whether the individual landscape metrics described the land cover patterns in ways that would facilitate comparisons of landscape patterns over time and large areas and in different land cover mapping products. We examined the spatial patterns in metrics in the original satellite image classification of land cover (called the "unsmoothed map" in this paper), and a smoothed satellite image classification map, which resembled the "polygon-based" map products used by S. Cushman and others in the MLEP (McGarigal, 2003; see also the Web site presentation available at http://www.umass.edu/landeco/presentations/plenary/index.html/). This comparison highlighted the differences in map characteristics (e.g., minimum mapping unit and map resolution) that are possible when considering different geospatial technologies to generalize landscape patterns and tested how these characteristics affect the prediction of universal and consistent structure gradients.

Study area and data collection

This study was carried out in the eastern portion of the Foothills Model Forest (Stenhouse and Munro, 2000), located within the Canadian Rocky Mountains Yellowhead Ecosystem, Alberta, Canada (**Figure 1**). The approximately 6000 km^2 foothills zone includes a range in elevation from about 900 to 1700 m. The upper (western) foothills are characterized by gently to strongly rolling hills dominated by conifer forests, and the lower (eastern) foothills have rolling hills with mixed conifer and deciduous forests and numerous wetlands. To capture the spatial patterns within the Foothills region, we subdivided this study area into 195 non-overlapping 5.4 km × 5.4 km sub-landscapes. This number and size of sub-landscape units are necessary to create an adequate three to one sample to metric ratio for a principal component analysis (McGarigal et al., 2000). We superimposed the square sub-landscapes on the land cover map and extracted 49 class-level and 54 landscape-level metrics also used in the MLEP project (Appendix A) using FRAGSTATS version 3.3 (McGarigal et al., 2002).

The land cover map used as the basis for this analysis was derived using an integrated decision tree approach (IDTA) on Landsat enhanced thematic mapper plus (ETM+) satellite imagery (Franklin et al., 2001). The IDTA method involves a judicious mix of unsupervised clustering and supervised classification procedures using field–training data applied to spectral variables and terrain variables extracted from a digital elevation model (DEM). Overall accuracy of the final map was determined to be approximately 80% correct, with varying user's and producer's accuracies for the individual 15 land cover classes (see Franklin et al., 2001 for details). The impact of map accuracy on landscape metric errors has been quantified in several studies. The findings ranged from no significant effects when land cover composition differences were less than 5% of the misclassification rates (Wickham et al., 1997) to relationships between map errors and metric errors being inversely (Shao et al., 2001) or nonlinearly related, with map smoothing techniques yielding lower map errors but higher metric errors (Langford et al., 2006). An analysis of the impact of map accuracy on derived structure gradients is another study that should be tested in the future. For this analysis, the original 15 IDTA land cover classes were regrouped into a more generalized classification scheme with eight land cover classes (**Table 1**; **Figure 1**) to ensure adequate representation of all classes in the 195 sub-landscapes. To simulate a polygon-based, GIS-like map such as used by the preliminary parsimony analysis, we applied a smoothing filter to the original IDTA map, increasing the minimum mapping unit from one to eight

Table 1. Generalized integrated decision tree approach (IDTA) land cover classes used in this landscape metric analysis.

Class	Description
1	Closed forest
2	Open forest
3	Herbaceous
4	Shrub
5	Bogs
6	Nonforested features
7	Linear features
8	Disturbed sites

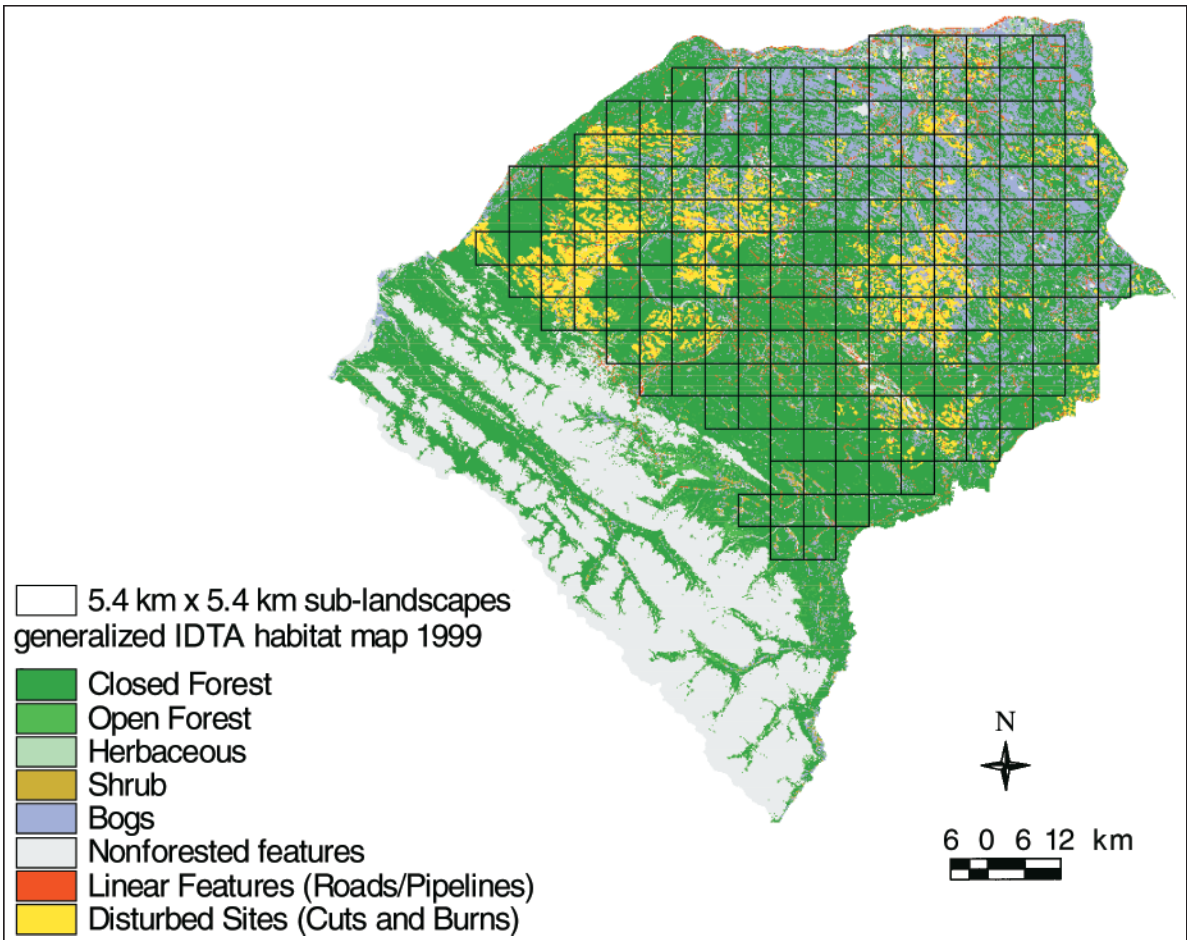

Figure 1. Stratification of the generalized IDTA foothills of the extended Grizzly Bear Research Project boundary for the purpose of the parsimony analysis.

30 m × 30 m pixels (**Figure 2**). This filter removes all patches less than the specified minimum mapping unit by replacing small patches with the majority inside a 3 × 3 window. The smoothed, polygon-based, generalized IDTA land cover map was used to identify the parsimonious structure gradients that exist in this Foothills region; a second objective was to compare these gradients with those suggested by S. Cushman, K. McGarigal, and M.C. Neel (personal communication, 2002). The unsmoothed original IDTA land cover map was subsequently used to investigate if the class-level parsimonious metrics suite was relatively insensitive to the input land cover map characteristics (for example, if their extraction was dependent on the grain and resolution of the maps used to obtain the individual landscape metrics).

Methods

For the smoothed and unsmoothed satellite image classification maps of the Foothills region land cover, we undertook the following four-step parsimony analysis for the class- and landscape-level metrics:

(1) Independent class-level structure gradients, composed of linear combinations of class-level landscape metrics, were generated for each of the eight generalized land cover classes using a partial principal component analysis on the correlation matrix of the 49 metrics. The function PROC FACTOR in SAS (SAS Institute Inc., 2002) was used. To remove the confounding effects of landscape composition on the resulting principal components of configuration metrics, the metric "Pland" (the proportion of land cover class) was statistically partialled out during this analysis. The latent root criterion was used to determine the number of significant principal components by dropping any components from further scrutiny with eigenvalues less than one (McGarigal et al., 2000).

(2) To identify principal components, or structure gradients, that were similar across the eight land cover classes, we applied a polythetic agglomerative hierarchical clustering technique with average linkage using the PROC CLUSTER function in SAS (SAS Institute Inc., 2002). In this analysis step, similarity of principal components was assessed by comparing their respective component loadings. A distance matrix needed to be created based on the computation of a Pearson's correlation matrix of all principal components (n = 75) across all classes. This correlation matrix was transformed to a distance matrix by subtracting each correlation coefficient $|r|$ from 1 to create distance values ranging from 0, indicating perfect correlation, to 1, indicating no correlation between the loadings of individual components. Cluster membership was based on the point of inflection of the scree plot of fusion distances (McGarigal et al., 2000). This cutoff occurred at a fusion distance of 0.69 with 16 structure gradients clusters for the unsmoothed satellite image

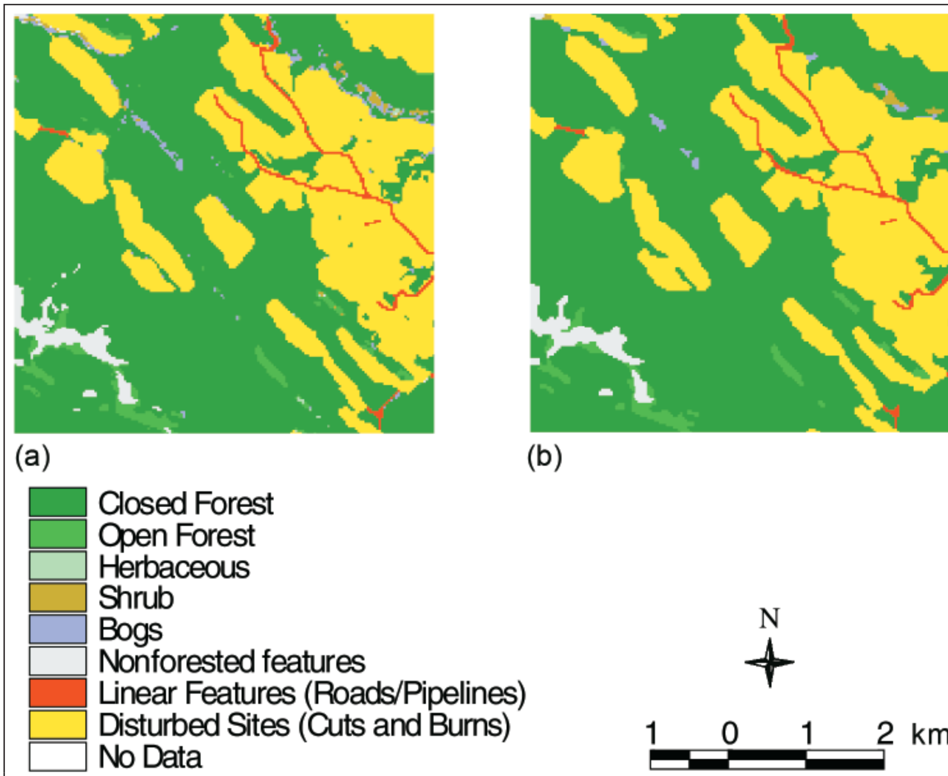

Figure 2. Land cover subset showing mapping details from (a) unsmoothed, generalized remote sensing derived IDTA land cover map; and (b) smoothed, generalized polygon-based, GIS-like IDTA land cover map.

classification map and at a fusion distance of 0.61 with 20 metric gradient clusters for the smoothed satellite image classification map.

(3) Independent landscape-level structure gradients were similarly produced on the two maps using a principal component analysis on the correlation matrix of the 54 landscape-level metrics using the function PROC FACTOR in SAS (SAS Institute Inc., 2002). We did not partial out any landscape metric in the landscape-level analysis, since there was no landscape-level metric comparable to Pland. We interpreted the contributing metrics the same way as that in the class-level analysis.

(4) We interpreted three measures to assess importance of the resulting principal components, now labelled appropriately as landscape structure gradients. *Universality* is the percentage of classes a particular landscape metric gradient occurred within; *consistency* is based on the average within-cluster Pearson's correlation among the loadings of the constituting components, or structure gradients, indicating the degree of stability of metric behaviour within a particular group (i.e., a consistent group is oriented in the same direction by the constituting metrics); and *strength* is based on the mean eigenvalue and mean explained variance per structure gradient cluster, indicating the average explanatory power of a given gradient. We identified landscape structure gradients as universal when 80%–100% universality was observed and as consistent when the within-cluster correlation of loadings was greater than 0.70. Although we report all three of these measures, universality and consistency were considered the primary indicators of metric importance. Landscape structure gradients made up of metrics with loadings greater than 0.40 or less than –0.40 on a given component were retained in the analysis. Greater emphasis in the interpretation was given to those metrics with loadings greater than 0.60 or less than –0.60 (McGarigal et al., 2000). The metrics describing a particular metric gradient were listed with their respective relationships indicated by positive and negative signs.

All class- and landscape-level structure gradients were compared with those found by earlier work from MLEP and assigned with their gradient number. Structure gradients unique to this analysis were assigned numbers above 24 for class-level gradients and above 17 for landscape-level gradients.

Results and analysis

Class-level structure gradients of smoothed satellite image classification map

The partial principal component analysis identified between nine and 11 independent gradients of landscape metrics per land cover class, yielding a total of 77 landscape structure gradients across all classes. These structure gradients explained between 86% and 89% of the total variance among all metrics calculated for each cover class. The clustering analysis identified 20 structure gradient clusters, which had a mean within-gradient cluster consistency of $r = 0.77$. Among the 20 clusters of structure gradients, 15 were identified as being very similar to those found by the preliminary work of the MLEP (**Table 2**). These 15 gradients included all seven fundamental structure gradients found to be universal, consistent, and strong in the MLEP study. The following discussion focuses mainly on these seven gradients because of their overall importance expressed through their ability to explain most of the variance among metrics of landscape structure (strength), their presence across all land cover classes (universality), and their consistent measure of the same attributes of landscape patterns (consistency).

Five of the seven fundamental gradients identified by the MLEP project were also universal, consistent, and strong in our analysis (gradients 1, 2, 3, 4, and 6; **Table 2**). The structure gradients "patch shape complexity" (gradients 2a and 2b; **Table 2**) and "aggregation" (gradients 3a and 3b; **Table 2**) were each split into two complementary class membership gradients in our analysis. The two remaining fundamental structure gradients, "patch dispersion" and "neighbourhood similarity" (gradients 5 and 7; **Table 2**), were not globally present in our analysis because their occurrence was class specific, as indicated by low universality scores (37.5% and 50.0%, respectively). While neighbourhood similarity constituted a highly consistent metric gradient specific to open forest, herbaceous, shrubs, and bog cover classes, patch dispersion displayed less stable behaviour (gradient 5; **Table 2**). Further inspection of the factor patterns of this particular gradient cluster revealed that patch dispersion was highly consistent for the closed forest and shrubland, but not for the linear features cover type.

Faintly reduced universality of two of the five fundamental landscape structure gradients within this analysis appeared to be triggered by their non-occurrence in two main cover classes, namely "closed forest" and "linear features" (gradients 1 and 4; **Table 2**). This could suggest the presence of unique spatial patterns within either of these two land cover classes. Further inspection of structure gradients identified in this study revealed the presence of three strong (mean eigenvalues > 10.0), class-specific structure gradients that measured attributes of patterns of one or both of these land cover classes. The gradient "shape and correlation length of large patches" measured patterns of the closed forest type (gradient 9; **Table 2**), and "core area complexity" and "splitting and cohesion" measured spatial aspects unique to the linear features type (gradients 21 and 29; **Table 2**).

Compared with the MLEP study, slight differences in metric composition were demonstrated in two fundamental gradients. "Large patch dominance" and "aggregation" gradients had the same basic composition as that identified by S. Cushman, K. McGarigal, and M.C. Neel (personal communication, 2002), with the exception of new metric additions, such as mean proximity index (Prox_Mn) (gradient 6; **Table 2**) for large

Table 2. Principal component clusters (landscape structure gradients) identified through partial principal component and clustering analysis on 49 class-level configuration metrics across eight land cover classes.

Landscape structure gradient No.	Label	Contributing metrics (metric composition)	Land cover class membership of gradient	Universality (%)	Consistency	Mean eigenvalue	Mean explained variance (%)
6	Large patch dominance	Area_Aw+, LPI+, Core_Aw+, Dcore_Aw+, Prox_Mn	All	100.0	0.85	11.82	23.19
4	Nearest neighbour	Enn_Mn+, Enn_Aw+	2, 3, 4, 5, 6, 7, 8	87.5	0.86	1.78	3.50
2a	Patch shape complexity	Shape_Mn+, Frac_Aw+, Frac_Mn+, Shape_Aw+, Gyrate_Mn+	2, 3, 4, 5, 6, 7, 8	87.5	0.80	4.66	9.14
1	Edge contrast	TECI+, Econ_Mn+, Econ_Aw+	1, 2, 3, 4, 5, 6, 8	87.5	0.79	2.77	5.43
3a	Aggregation	Pladj+, Para_Aw-, Cohesion+, AI+, Clumpy+	2, 3, 4, 5, 6, 8	75.0	0.81	5.82	11.42
11	Patch size variability	Core_Cv+, Area_Cv+, Dcore_Cv+, Prox_Cv+	2, 3, 4, 5, 6, 8	75.0	0.77	7.81	15.32
25	Proximity and similarity	Prox_Mn+, Prox_Aw+, Simi_Mn+, Simi_Aw+	1, 2, 6, 7, 8	62.5	0.71	2.22	4.35
7	Neighbourhood similarity	Simi_Mn+, Simi_Aw+, Simi_Cv-	2, 3, 4, 5	50.0	0.81	2.19	4.29
26	Aggregation and splitting	Ai+, Split+, Clumpy+	2, 3, 4, 6	50.0	0.76	1.45	2.86
13	Edge–patch density	DCAD+, PD+, CWED+, ED+, LSI+	3, 5, 8	37.5	0.84	3.29	6.45
27	Variability in perimeter–area ratio and core area index	CAI_Cv+, Para_Cv+	1, 5, 8	37.5	0.76	1.55	3.03
3b	Aggregation	AI-, Clumpy- Pladj-, Para_AW+	1, 7, 8	37.5	0.76	5.69	11.16
5	Patch dispersion	Enn_Cv	1, 4, 7	37.5	0.49	1.16	2.27
28	Core area index	CAI_Mn+, CAI_Aw+	4, 6	25.0	0.86	1.64	3.22
9	Shape and correlation length of large patches	Frac_Aw+, Shape_Aw+, Shape_Cv+, Gyrate_Cv+, Gyrate_Aw+	1, 5	25.0	0.80	5.24	10.27
2b	Patch shape complexity	Shape_Mn+, Frac_Mn+	1, 7	25.0	0.64	5.47	10.70
29	Core area complexity	Core_Mn+, Core_Aw+, Dcore_Aw+, Dcore_Mn+, CAI_Aw+, Dcore_Cv+	7	12.5	na	9.83	19.23
21	Splitting and cohesion	Split-, Cohesion+, Econ_Aw+, TECI+	7	12.5	na	5.57	10.93
12	Proximity index coefficient of variation	Prox_Cv+	1	12.5	na	1.36	2.67
10	Perimeter-area coefficient of variation	Para_Cv+	6	12.5	na	1.07	2.10

Note: Consistency was assessed against the average of all within-cluster correlations across all classes (r = 0.77). na, not applicable.

patch dominance, and area-weighted perimeter to area ratio (PARA_Aw) for aggregation (gradient 3; **Table 2**). These new metric additions appear to be important descriptors of this particular landscape. In the earlier work in different study areas, the area-weighted proximity index (Prox_Aw) and the mean perimeter to area ratio (PARA_Mn) were separate, independent gradients with similarly high universality scores.

Besides the new metric additions to some fundamental gradients in this study, we identified some other unique structure gradients. Five highly consistent gradients existed that were specific to certain land cover classes (gradients 25–29; **Table 2**). "Proximity" and "variability in perimeter to area ratio coefficient" were independent, separate gradients in the MLEP study (S. Cushman, K. McGarigal, and M.C. Neel, personal communication, 2002), but they co-occurred with "similarity" (gradient 25; **Table 2**), and "core area index coefficient of variation" (gradient 27, **Table 2**), respectively, in this analysis. Aggregation formed a third, new and independent gradient in conjunction with “splitting index” (gradient 26; **Table 2**), and core area index (gradient 28, **Table 2**) and core area complexity (gradient 29, **Table 2**) have not previously been identified.

Comparison of class-level structure gradients of unsmoothed satellite image classification maps with those of smoothed satellite image classification maps

The partial principal component analysis applied to the unsmoothed satellite image classification map product again identified between nine and 11 independent gradients of landscape metrics for each of the eight generalized land cover classes, yielding a total of 75 structure gradients across all classes. The structure gradients explained between 86% and 88% of the variance among all 49 class-level metrics for each cover class. The clustering analysis identified only 16 structure gradient clusters, which had a mean within-gradient cluster consistency with no significant difference to that obtained in the smoothed land cover map analysis. We found the majority of gradients (13 of the total of 16 structure gradients) again to be very similar to those identified in the MLEP study. The three other gradients unique to this foothills landscape contained the same metric composition as those in the smoothed map (gradients 25, 28, and 29; **Table 2**).

Although all seven fundamental gradients existed as independent attributes of spatial pattern in the smoothed map, only five of these gradients occurred in the same metric composition in the unsmoothed analysis. Among these, “large patch dominance”, “nearest neighbour”, and “edge contrast” (gradients 1, 4, and 6; **Table 2**) occurred universally and consistently in the unsmoothed analysis, and “aggregation” (gradient 3; **Table 2**) and “patch shape complexity” (gradient 2; **Table 2**) occurred as highly consistent but more land cover class specific gradients. The metric composition for the remaining two fundamental gradients found in the smoothed analysis differed in the unsmoothed analysis. “Patch dispersion” was joined together with “proximity index coefficient of variation” (gradients 5 and 12), and “neighbourhood similarity” coexisted with “area-weighted proximity” (gradients 7 and 8). The closed forest and the linear features land cover types again seemed to be responsible for reducing the universality within the fundamental set of gradients, and five particularly strong but class-specific structure gradients, occurring frequently within these cover types, were noted. These gradients were nearly the same as those found in the smoothed map when present, such as “shape and correlation length of large patches” (gradient 9; **Table 2**), “aggregation and edge” (absent; **Table 2**), “mean patch size” (absent; **Table 2**), “splitting and cohesion” (gradient 21; **Table 2**), and “core area complexity” (gradient 29; **Table 2**).

In summary, several aspects in the unsmoothed map analysis were different from those in the smoothed map analysis. The main differences in the unsmoothed map analysis were the slightly lower number of components and the lower number of clusters or structure gradients. Only three gradients of the fundamental set were found to be universal and consistent in this analysis compared with five in the smoothed map analysis. All deviations in the gradient composition between the smoothed and unsmoothed satellite image classification maps were interpreted to be a function of the smaller minimum mapping unit in the case of the unsmoothed map analysis. Other studies have already demonstrated that absolute values of metrics from the same area and time cannot be compared when they originate from maps produced using different geospatial technologies, such as aerial photograph interpretation or “polygon-based maps” versus individual “pixellated” map products such as those readily generated using satellite image classification techniques (e.g., Franklin et al., 2002). The effect of the spatial patterns associated with the smallest patches in “pixellated” map products of the same landscape was demonstrated in the metric composition of the fundamental structure gradient “patch dispersion”. Although occurring independently of other metrics in the smoothed analysis, “patch dispersion” (gradient 5; **Table 2**) occurred in combination with the “proximity index coefficient of variation” in the unsmoothed analysis. Such a positive association between “patch dispersion” and “proximity index coefficient of variation” indicates that low variability in interpatch distances in a landscape is associated with a low variability in the proximity index of the same patches, and vice versa. Since the minimum mapping unit was equated to the grain (individual pixels) in the unsmoothed analysis, areas with lower spatial homogeneity gave rise to individual small, one or a few pixel patches of the same land cover type in close proximity to each other (i.e., hence increasing the variability in mean nearest neighbour distances simultaneously with an increase in the variability of patch proximity). In the smoothed, polygon-based analysis, the minimum mapping unit was much larger than the grain, and areas of lower homogeneity were generalized and assigned to the dominant surrounding patch type, and patch dispersion therefore became less affected by the variability in patch proximity. Overall, however, our parsimony analysis suggested that the interrelationships between the behaviour of most metrics on the unsmoothed map were very similar to the behaviour of those metrics observed on the smoothed map.

Validating the existence of fundamental class-level structure gradients

The parsimony analysis in the Foothills region supported the interpretation (S. Cushman, K. McGarigal, and M.C. Neel, personal communication, 2002) that seven fundamental class-level structure gradients exist across broad areas of North America and that these fundamental gradients universally and consistently describe the major attributes of landscape structure. All seven gradients occurred within the Foothills region, together explaining on average approximately 59% of all class-level variation, when present. Five of the seven fundamental gradients were universal and consistent across all cover types. The five fundamental gradients universal within this analysis (gradients 1, 2, 3, 4, and 6; **Table 2**) carried most

Table 3. Six significant principal components or landscape structure gradients of 54 landscape-level configuration metrics as retained from principal component analysis.

Landscape structure gradient No.	Label	Contributing metrics (metric compostion)	Cushman gradient similarity	Cumulative explained variance (%)
1	Contagion–diversity	ED-, LSI-, Pladj+, Para_Aw-, Dcore_Mn+, Core_Mn+, DCAD-, Clumpy+, AI+, Area_Mn+, CAI_Mn+, PD-, CWED-, ENN_Mn+	Similar	54
4	Edge contrast	ECON_Aw+, ECON_Mn+TECI+, SIMI_Cv+	Same except for the lack of patch richness density (PRD)	66
18	Interspersion – patch shape	IJI-, Shape_Mn+, FRAC_Mn+, Frac_Cv+	Different	76
2	Large patch dominance	Dcore_Cv+, Core_Cv+, Area_Cv+, LPI+, Shape_Aw+, Split-, Gyrate_Aw+	Same	81
9	Area-weighted proximity	Prox_Aw	Same	84
8	Patch dispersion	Enn_Cv	Same	86

Note: Components are ordered by their explanatory power (percent explained variance). The meaning of each component is provided by the metric gradient name, listing also the largest positive and negative loadings.

of the explanatory power (about 52%), reinforcing an interpretation of their particular importance for all cover types of the Foothills region. The fact that overall 15 of the 20 gradients were very similar to those identified by the earlier work undertaken by the MLEP supports the conclusion that there are several major dimensions of landscape pattern and that these gradients reflect consistent interrelationships among metrics across a broad range of land cover classes.

The parsimony analysis in the original unsmoothed satellite image classification map supported the notion that the same general interrelationships among metrics existed regardless of the geospatial technology used to generate the input data layers. A total of 13 of the 16 gradients were identified as being very similar to those identified by the gradients from the other regions. Only five of the fundamental seven gradients identified by the MLEP study were present in the unsmoothed map analysis, but they carried a strong joined explanatory power; on average, 61% of all class-level variation was explained by these five fundamental gradients when present in the given cover type. The three fundamental gradients also universal within this unsmoothed map analysis (“large patch dominance”, “nearest neighbour”, “edge contrast”) carried approximately 32% of the explanatory power for all classes, reiterating their importance for all cover types of the Foothills region. This result, however, also signified a general reminder that the fundamental structure gradients do not suffice to capture all spatial aspects of a landscape. To explain a higher portion of the class-level variation, consistent structure gradients, which were specific to certain cover classes (e.g., gradients 9 and 21; **Table 2**) or specific to a certain landscape (gradients 25–29; **Table 2**), needed to be considered in an analysis of landscape structure. Although generally the structure gradients had high similarity, there were fewer gradients in the Foothills region compared with the gradients derived from the landscapes analyzed by the MLEP. Fewer gradients were identified to capture similar total amounts of variation among metrics of the Foothills landscape, suggesting a slightly lower spatial complexity (i.e., 20 gradients over all classes, based on 9–11 gradients per class, in the Foothills landscape compared with 24 overall gradients in the MLEP study, based on 12–15 gradients per class) than in the other three landscapes.

The main difference in the two studies lies in the fact that the Foothills study was based on satellite image classification maps, whereas the earlier work relied on existing maps contained in polygonal GIS databases. We applied a smoothing filter to increase the grain in our study area, and this appeared to create a map database more similar to a polygon-based map. A second difference involved the size of the sub-landscapes analyzed for structure gradients. A reduction in sub-landscape extent in the Foothills from 7.6 km × 7.6 km squares to 5.4 km × 5.4 km squares did not appear to affect the analysis. The seven fundamental gradients were still present. We therefore assumed that any differences between the gradients found in this region in comparison to the other regions are scale independent and are an expression of the unique landscape characteristics of the Foothills region.

Landscape-level landscape structure gradients of smoothed satellite image classification map

The principal component analysis retained six components, or structure gradients, together explaining 86% of the variance in the 54 landscape-level metrics across 195 landscapes (**Table 3**). This result stood in slight contrast to the three landscapes analyzed of the MLEP, where a similar amount of variance among landscape metrics was explained (88%–94%), but with a considerably higher number of gradients (10–14 structure gradients), suggesting again a lower diversity of spatial attributes inherent in the foothills landscape than in the landscapes of the MLEP. Among the identified six gradients, however, five were similar to the landscape-level gradients identified by the MLEP (gradients 1, 2, 4, 8, and 9; **Table 3**) and four belonged to the eight fundamental landscape-level gradients (gradients 1, 2, 4, and 8; **Table 3**). The gradient “contagion” was identified as being the strongest landscape-level structure gradient by explaining more than 50% of the variance among the landscape metrics (gradient 1; **Table 3**), which is similar to its importance in the MLEP study, where it was also the strongest gradient, with an average explanatory power of 34%.

The remaining four fundamental structure gradients identified by the MLEP study were not present here independently. “Patch shape variability”, “mean proximity”, and “nearest neighbour distance” (fundamental gradients 5, 6, and 7) were missing completely, and “interspersion” (fundamental gradient 3) occurred in combination with “patch shape” (MLEP gradient 10), together forming a unique, sixth gradient (gradient 18; **Table 3**).

Comparison of landscape-level structure gradients of unsmoothed satellite image classification maps with those of smoothed satellite image classification maps

Six structure gradients were also retained in the unsmoothed land cover map, which together explained 2% more of the total variation (88% total explained variance) in the 54 landscape-level metrics across 195 landscapes than in the unsmoothed analysis. The gradients extracted from the unsmoothed and smoothed land cover maps were similar in that four gradients (gradients 1, 2, 4, 9) contained the same metric composition. In addition, among these four gradients, “contagion” was again the strongest landscape-level gradient, explaining 53% of the variance among landscape metrics of the unsmoothed map (gradient 1). Two of the landscape-level gradients were different between the two analyses. Although the fundamental gradient “patch dispersion” (gradient 8) had occurred as an independent gradient in the smoothed analysis, it occurred in combination with the fundamental gradient “interspersion” (fundamental gradient 3) in the unsmoothed analysis. In contrast, although “patch shape” (fundamental gradient 10) occurred in combination with “interspersion” in the smoothed analysis (gradient 18; **Table 3**), it occurred as an independent gradient in the unsmoothed analysis, similar to the case in the MLEP study. Overall, the same pool of structure gradients (gradients 1, 2, 3, 4, 8, 9, and 10) occurred in both map analyses of the foothills landscape, with the only difference existing in different combinations of gradients 3, 8, and 10 across the two analyses; in the unsmoothed analysis, “patch shape” was replaced by “patch dispersion” in the joined gradient with “interspersion”, and “patch shape” was identified as an independent gradient.

A clear example of the smoothed and unsmoothed mapping technique results is that “patch shape” is an independent attribute of spatial pattern in the unsmoothed map analysis but not in the smoothed analysis. Both mapping techniques assessed the same shapes of landscape patches larger than the minimum mapping unit of 8 pixels × 8 pixels, but only the unsmoothed analysis captured patch shapes between 1 pixel and 64 (8 × 8) pixels. These shapes included highly regular, perfectly square, and compact patch shapes due to the shape of a pixel. Although patch shapes above the minimum size for the smoothed map seemed to be highly interrelated with the spatial interspersion of patches of the same land cover type in this foothills landscape (i.e., indicating that patch shape grew more irregular with increasingly disproportional distribution of patches, gradient 18; **Table 3**), patch shape constituted an independent attribute of spatial pattern in unsmoothed analysis. The highly regular, compact shape of patches the size of individual pixels therefore overshadowed the general spatial characteristics of this particular landscape (i.e., the trend that patch shape increased in irregularity the more disproportionately the patches were distributed) solely as a function of the mapping technique.

Validating the existence of fundamental landscape-level structure gradients

A large portion of variance among landscape metrics describing the Foothills region could be characterized by very few structure gradients able to explain most of the variation. With the exception of the gradients “patch shape variability”, “mean proximity index”, and “nearest neighbour distance”, the other five fundamental landscape-level structure gradients existed in either the same composition or in combination with other gradients. “Contagion” was the strongest gradient in the foothills landscape (gradient 1; **Table 3**) and in the landscapes analyzed by the MLEP study.

These findings strongly support the universality and consistency of the eight fundamental landscape-level gradients. For the smoothed map, a metric representative of each fundamental gradient would have entirely sufficed to capture at least 84% of the landscape-level spatial variation. This fundamental set introduced some redundancy, however, since “mean proximity”, “patch shape variability”, and “nearest neighbour distance” did not have any explanatory power in the Foothills region, but rather described similar aspects of spatial patterns, as did other gradients. On the other hand, in the Foothills region, “area-weighted proximity” would have been missed by using only the fundamental set of gradients, but the effects would likely be of minor significance because this gradient only explained approximately 3% of the landscape-level patterns.

The eight fundamental landscape-level structure gradients would also have sufficed to describe most of the foothills landscape pattern variation when considering the unsmoothed map product. The explanatory power of the fundamental gradients was slightly lower (75%) for the unsmoothed map than for the smoothed foothills landscape map, however, because of the strong independent gradient “patch shape” (11% average explanatory power, gradient 10). As stated in the previous section, the reduction in minimum mapping unit and the geometry of the smallest units (square pixels) in the unsmoothed map analysis caused a significant reduction in patch shape index, representing more compact and less irregularly shaped patches in comparison to the polygon-based, smoothed map analysis where “patch shape” had been interdependent with interspersion (gradient 18; **Table 3**).

“Patch shape” appeared in the MLEP study, but it was not in the fundamental set of structure gradients. Although the fundamental set of eight landscape-level gradients would have not accounted for the explanatory power of “patch shape” (11% explained variance), missing the “area-weighted proximity” (gradient 9; **Table 3**) by using only the fundamental gradient set would again be of only minor significance, since this gradient only explained approximately 2% of the landscape-level patterns.

Would the fundamental structure gradients identified by the MLEP study also explain most aspects of spatial patterns of the same landscape if there were more land cover classes? The MLEP structure gradients were based on three different land cover maps with four, five, and seven land cover types. The high overall correspondence between the structure gradients of the foothills structure and the MLEP landscapes suggested validation of the existence of fundamental landscape-level gradients across different landscapes, mapped in ranges of four to eight land cover classes. The effect of increasing the categorical detail with a greater number of land cover classes remains a question to be tested in the future.

Conclusion

We compared structure gradients in smoothed and unsmoothed satellite image classification maps to determine a parsimonious, fundamental suite of metrics useful in quantifying and comparing landscapes over time and with different geospatial mapping products. Analysis at the class and landscape level, using both smoothed and unsmoothed maps, supports the existence of several fundamental structure gradients. These structure gradients constitute consistent combinations of specific landscape metrics that universally describe the major attributes of landscape configuration. Seven fundamental class-level structure gradients occurred within this region and together explain the majority of all class-level variation (on average approximately 59% when all present per given cover type, and about 53% for all cover types). The landscape-level analysis demonstrated that eight fundamental landscape-level structure gradients explained about 85% of the variance. These findings confirm the suggestions from the preliminary work by MLEP that these structure gradients are universal, consistent, and strong, and they could form the minimum set of landscape metrics required to describe the spatial patterns in any landscape.

Acknowledgements

This work was funded by the Natural Sciences and Engineering Research Council of Canada (NSERC) through a Collaborative Research and Development Award. We are very grateful for additional support from the many partners of the Foothills Model Forest Grizzly Bear Research Project. Julia Linke was supported by an Alberta Ingenuity Fund stipend and by an NSERC scholarship. The earlier work and comments by S. Cushman, M. Neel, and K. McGarigal were important to the success of our work. We thank S. Bertazzon, G. Castilla, M. Hall-Beyer, F. Huettmann, K. McGarigal, and two independent reviewers for very helpful contributions to this manuscript.

Reference

Chapin, T.G., Harrison, D.J., and Katnik, D.D. 1998. Influence of landscape pattern on habitat use by American Marten in an industrial forest. *Conservation Biology*, Vol. 12, No. 6, pp. 1327–1337.

Davidson, C. 1998. Issues in measuring landscape fragmentation. *Wildlife Society Bulletin*, Vol. 26, No. 1, pp. 32–37.

Diaz, N.M. 1996. Landscape metrics: a new tool for forest ecologists. *Journal of Forestry*, Vol. 94, No. 12, pp. 12–16.

Franklin, S.E., Dickson, E.E., Farr, D.R., Hansen, M.J., and Moskal, L.M. 2000. Quantification of landscape change from satellite remote sensing. *The Forestry Chronicle*, Vol. 76, No. 6, pp. 877–886.

Franklin, S.E., Stenhouse, G.B., Hansen, M.J., Popplewell, C.C., Dechka, J.A., and Peddle, D.R. 2001. An integrated decision tree approach (IDTA) to mapping landcover using satellite remote sensing in support of grizzly bear habitat analysis in the Alberta Yellowhead Ecosystem. *Canadian Journal of Remote Sensing*, Vol. 27, No. 6, pp. 579–591.

Franklin, S.E., Hansen, M.J., and Stenhouse, G.B. 2002. Quantifying landscape structure with vegetation inventory maps and remote sensing. *The Forestry Chronicle*, Vol. 78, No. 6, pp. 866–875.

Frohn, R.C. 1998. *Remote sensing for landscape ecology. New metric indicators for monitoring, modeling, and assessment of ecosystems*. Lewis Publishers, New York.

Knutson, M.G., Sauer, J.R., Olsen, D.A., Mossman, M.J., Hemesath, L.M., and Lannoo, M.J. 1999. Effects of landscape composition and wetland fragmentation on frog and toad abundance and species richness in Iowa and Wisconsin, U.S.A. *Conservation Biology*, Vol. 13, No. 6, pp. 1437–1446.

Langford, W.T., Geregel, S.E., Dietterich, T.G., and Cohen, W. 2006. Map misclassification can cause large errors in landscape pattern indices: examples from habitat fragmentation. *Ecosystems*, Vol. 9, pp. 474–488.

Levin, S.A. 1992. The problem of patterns and scale in ecology. *Ecology*, Vol. 73, No. 6, pp. 1943–1967.

Linke, J., Franklin, S.E., Huettmann, F., and Stenhouse, G.B. 2005. Seismic cutlines, changing landscape metrics and grizzly bear landscape use in Alberta. *Landscape Ecology*, Vol. 20, No. 7, pp. 811–826.

McGarigal, K. 2003. Evolving science and application of landscape analysis. In *Proceedings of the 6th Annual IALE World Congress Plenary Session*, 13–17 August 2003, Darwin, Australia. Available from http://www.umass.edu/landeco/presentations/plenary/index.html [accessed 16 January 2007].

McGarigal, K., and Marks, B.J. 1995. *FRAGSTATS. Spatial pattern analysis program for quantifying landscape structure*. General Technical Report PNW-GTR-351, Pacific Northwest Research Station, US Department of Agriculture, Forest Service, Portland, Oreg. 122 pp.

McGarigal, K., and McComb, W.C. 1995. Relationship between landscape structure and breeding birds in the Oregon Coast Range. *Ecological Monographs*, Vol. 65, pp. 235–260.

McGarigal, K., Cushman, S.A., and Stafford, S. 2000. *Multivariate statistics for wildlife and ecology research*. Springer-Verlag, New York.

McGarigal, K., Cushman, S.A., Neel, M.C., and Ene, E. 2002. *FRAGSTATS: spatial pattern analysis program for categorical maps*. Computer software program produced by the authors at the University of Massachusetts, Amherst, Mass. Available from www.umass.edu/landeco/research/fragstats/fragstats.html [accessed 16 January 2007].

Potvin, F., Lowell, K., Fortin, M.-J., and Belanger, L. 2001. How to test habitat selection at the home range scale: a resampling random windows technique. *Ecoscience*, Vol. 8, No. 3, pp. 399–406.

Riitters, K.H., O'Neill, R.V., Hunsaker, C.T., Wickham, J.D., Yankee, D.H., Timmins, S.P., Jones, K.B., and Jackson, B.L. 1995. A factor analysis of landscape pattern and structure metrics. *Landscape Ecology*, Vol. 10, No. 1, pp. 23–39.

SAS Institute Inc. 2002. *SAS system*. SAS Institute Inc., Cary, N.C.

Shao, G., Liu, D., and Zhao, G. 2001. Relationships of image classification accuracy and variation of landscape statistics. *Canadian Journal of Remote Sensing*, Vol. 27, No. 1, pp. 33–43.

Stenhouse, G., and Munro, R. 2000. *Foothills Model Forest Grizzly Bear Research Program 2000 annual workplan (year 2)*. Foothills Model Forest, Hinton, Alta.

Stuart-Smith, A.K., Bradshaw, C.J.A., Boutin, S., Hebert, D.M., and Rippin, A.B. 1997. Woodland caribou relative to landscape patterns in northwest Alberta. *Journal of Wildlife Management*, Vol. 61, No. 3, pp. 623–633.

Wickham, J.D., O'Neill, R.V., Riitters, K.H., Wade, T.G., and Jones, K.B. 1997. Sensitivity of landscape metrics to land-cover misclassification and differences in land-cover composition. *Photogrammetric Engineering and Remote Sensing*, Vol. 63, No. 4, pp. 397–402.

Wiens, J.A. 1989. Spatial scaling in ecology. *Functional Ecology*, Vol. 3, pp. 385–397.

Appendix A appears on the following page.

Appendix A

Table A1. List of 49 class-level (C) and 54 landscape-level (L) metrics computed in this paper.

Metric No.	Level	Acronym	Name
0	C	PLAND	Proportion of landscape
1	C, L	PD	Patch density
2	C, L	LPI	Largest patch index
3	C, L	ED	Edge density
4	C, L	LSI	Landscape shape index
5	C, L	AREA_MN	Mean patch size
6	C, L	AREA_AM	Area-weighted mean patch size
7	C, L	AREA_CV	Patch size coefficient of variation
8	C, L	GYRATE_MN	Mean radius of gyration
9	C, L	GYRATE_AM	Correlation length
10	C, L	GYRATE_CV	Radius of gyration coefficient of variation
11	C, L	SHAPE_MN	Mean shape index
12	C, L	SHAPE_AM	Area-weighted mean shape index
13	C, L	SHAPE_CV	Shape index coefficient of variation
14	C, L	FRAC_MN	Mean fractal dimension
15	C, L	FRAC_AM	Area-weighted mean fractal dimension
16	C, L	FRAC_CV	Fractal dimension coefficient of variation
17	C, L	PARA_MN	Mean perimeter–area ratio
18	C, L	PARA_AM	Area-weighted mean perimeter–area ratio
19	C, L	PARA_CV	Perimeter–area ratio coefficient of variation
20	C, L	DCAD	Disjunct core area density
21	C, L	CORE_MN	Mean core area
22	C, L	CORE_AM	Area-weighted mean core area
23	C, L	CORE_CV	Core area coefficient of variation
24	C, L	DCORE_MN	Mean disjunct core area
25	C, L	DCORE_AM	Area-weighted mean disjunct core area
26	C, L	DCORE_CV	Disjunct core area coefficient of variation
27	C, L	CAI_MN	Mean core area index
28	C, L	CAI_AM	Area-weighted mean core area index
29	C, L	CAI_CV	Core area coefficient of variation
30	C, L	PROX_MN	Mean proximity index
31	C, L	PROX_AM	Area-weighted mean proximity index
32	C, L	PROX_CV	Proximity index coefficient of variation
33	C, L	SIMI_MN	Mean similarity index
34	C, L	SIMI_AM	Area-weighted mean similarity index
35	C, L	SIMI_CV	Similarity coefficient of variation
36	C, L	MNN_MN	Mean nearest neighbour distance
37	C, L	MNN_AM	Area-weighted mean nearest neighbour distance
38	C, L	MNN_CV	Nearest neighbour distance coefficient of variation
39	C, L	CWED	Contrast-weighted edge density
40	C, L	TECI	Total edge contrast index
41	C, L	ECON_MN	Mean edge contrast
42	C, L	ECON_AM	Area-weighted mean edge contrast
43	C, L	ECON_CV	Edge contrast coefficient of variation
44	C, L	CLUMPY	Clumpiness index
45	C, L	PLADJ	Proportion of like adjacencies
46	C, L	IJI	Interspersion–juxtaposition index
47	C, L	COHESION	Patch cohesion
48	C, L	SPLIT	Splitting index

Table A1 (*concluded*).

Metric No.	Level	Acronym	Name
49	C, L	AI	Aggregation index
50	L	MESH	Mesh size
51	L	DIVISION	Division index
52	L	PRD	Patch richness density
53	L	SIDI	Simpson's patch diversity
54	L	SIEI	Simpson's patch evenness